

RESEARCH ARTICLE | JANUARY 24 2023

## *In situ* uniaxial pressure cell for x-ray and neutron scattering experiments

G. Simutis ; A. Bollhalder; M. Zolliker ; J. Küspert ; Q. Wang ; D. Das ; F. Van Leeuwen ; O. Ivashko ; O. Gutowski; J. Philippe ; T. Kracht ; P. Glaevecke; T. Adachi ; M. v. Zimmermann; S. Van Petegem ; H. Luetkens ; Z. Guguchia ; J. Chang; Y. Sassa; M. Bartkowiak ; M. Janoschek 





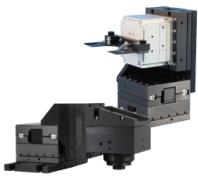
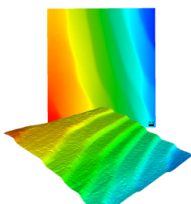
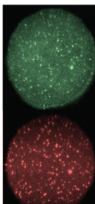
Rev Sci Instrum 94, 013906 (2023)

<https://doi.org/10.1063/5.0114892>



CrossMark

11 July 2023 07:17:15

 <b>MCL</b> MAD CITY LABS INC. <a href="http://www.madcitylabs.com">www.madcitylabs.com</a>	<p>Nanopositioning Systems</p> 	<p>Modular Motion Control</p> 	<p>AFM and NSOM Instruments</p> 	<p>Single Molecule Microscopes</p> 
---	--	--	---	--

# *In situ* uniaxial pressure cell for x-ray and neutron scattering experiments

Cite as: Rev. Sci. Instrum. 94, 013906 (2023); doi: 10.1063/5.0114892

Submitted: 26 July 2022 • Accepted: 24 December 2022 •

Published Online: 24 January 2023



G. Simutis,<sup>1,2,a</sup> A. Bollhalder,<sup>1</sup> M. Zolliker,<sup>1</sup> J. Küspert,<sup>3</sup> Q. Wang,<sup>3</sup> D. Das,<sup>4</sup> F. Van Leeuwen,<sup>1,5</sup> O. Ivashko,<sup>6</sup> O. Gutowski,<sup>6</sup> J. Philippe,<sup>1,3</sup> T. Kracht,<sup>6</sup> P. Glaeveccke,<sup>6</sup> T. Adachi,<sup>7</sup> M. v. Zimmermann,<sup>6</sup> S. Van Petegem,<sup>5</sup> H. Luetkens,<sup>4</sup> Z. Guguchia,<sup>4</sup> J. Chang,<sup>3</sup> Y. Sassa,<sup>2</sup> M. Bartkowiak,<sup>1</sup> and M. Janoschek<sup>1,3</sup>

## AFFILIATIONS

<sup>1</sup>Laboratory for Neutron and Muon Instrumentation, Paul Scherrer Institut, CH-5232 Villigen PSI, Switzerland

<sup>2</sup>Department of Physics, Chalmers University of Technology, SE-41296 Göteborg, Sweden

<sup>3</sup>Physik-Institut, Universität Zürich, Winterthurerstrasse 190, CH-8057 Zürich, Switzerland

<sup>4</sup>Laboratory for Muon Spin Spectroscopy, Paul Scherrer Institute, Villigen PSI, Switzerland

<sup>5</sup>Structure and Mechanics of Advanced Materials, Paul Scherrer Institut, CH-5232 Villigen PSI, Switzerland

<sup>6</sup>Deutsches Elektronen-Synchrotron DESY, Notkestraße 85, 22607 Hamburg, Germany

<sup>7</sup>Department of Engineering and Applied Sciences, Sophia University, Chiyoda, Tokyo, 102-8554, Japan

<sup>a</sup>Author to whom correspondence should be addressed: [gediminas.simutis@psi.ch](mailto:gediminas.simutis@psi.ch)

## ABSTRACT

We present an *in situ* uniaxial pressure device optimized for small angle x-ray and neutron scattering experiments at low-temperatures and high magnetic fields. A stepper motor generates force, which is transmitted to the sample via a rod with an integrated transducer that continuously monitors the force. The device has been designed to generate forces up to 200 N in both compressive and tensile configurations, and a feedback control allows operating the system in a continuous-pressure mode as the temperature is changed. The uniaxial pressure device can be used for various instruments and multiple cryostats through simple and exchangeable adapters. It is compatible with multiple sample holders, which can be easily changed depending on the sample properties and the desired experiment and allow rapid sample changes.

© 2023 Author(s). All article content, except where otherwise noted, is licensed under a Creative Commons Attribution (CC BY) license (<http://creativecommons.org/licenses/by/4.0/>). <https://doi.org/10.1063/5.0114892>

## I. INTRODUCTION

In modern condensed matter physics, the understanding and control of collective quantum behavior is at the forefront of fundamental research. At the same time, it is the driver for future technologies with potential applications of quantum matter ranging from quantum computation and cryptography to energy harvesting and dissipationless electricity transfer in superconductors.<sup>1–4</sup>

Much of the interest in quantum matter arises from the ability to efficiently tune and switch its properties using external perturbations. This “tunability” is a result of quantum phases typically emerging due to the delicate interplay of several atomic-scale interactions.<sup>5,6</sup> Unconventional superconductivity is perhaps the

best-known example of a macroscopic quantum phase. Notably, extensive experimental studies carried out over the last few decades have highlighted that many quantum materials may be tuned toward a zero-temperature magnetic instability using external control parameters such as chemical substitution, hydrostatic pressure, or magnetic field, where the associated quantum fluctuations are generally believed to mediate superconductivity.<sup>7</sup>

Over the last decade, and in addition to these well-established tuning parameters, the uniaxial pressure (or strain) has been established as a crucial tool, which aided in revealing and understanding a series of remarkable new quantum states. In many correlated-electron systems with multiple interacting degrees of freedom (charge, spin, and lattice), quantum states are energetically

nearly degenerate and even minuscule external changes, especially in the form of uniaxial pressure, can modify the emergent properties substantially.<sup>8–16</sup> For example, the uniaxial pressure was exploited to unveil the complex superconducting pairing symmetry of  $\text{Sr}_2\text{RuO}_4$ .<sup>17–19</sup> Most recently, the uniaxial pressure has enabled studying the nature of the charge and spin density waves as well as their interplay with superconductivity in cuprates. In  $\text{YBa}_2\text{Cu}_3\text{O}_{7-x}$ , the uniaxial pressure was found to induce the zero-magnetic-field three-dimensional charge ordering,<sup>20,21</sup> while in  $\text{La}_{2-x}\text{Sr}_x\text{CuO}_4$ , it enables repopulation of the stripe order domains.<sup>22–24</sup> In  $\text{La}_{2-x}\text{Ba}_x\text{CuO}_4$ , an extremely low uniaxial stress induces a threefold increase in the onset of three dimensional superconductivity. The 3D superconducting coherence was shown to be anti-correlated with the large-volume-fraction spin-stripe order, and the relative prominence of the two phases can be regulated by using the uniaxial pressure.<sup>15,25</sup> In a broader view of quantum materials, the strain has also been suggested to stabilize exotic phases ranging from the enigmatic “hidden order”<sup>26</sup> to quantum spin liquids<sup>27</sup> to skyrmion lattices,<sup>11,28</sup> which are thought to be relevant for novel spintronics and memory applications.<sup>29</sup>

Recently, there has been tremendous progress in lab-based uniaxial devices based on piezoelectric stacks. In particular, devices based on the developments described in Ref. 30 have been commercialized and used in laboratories worldwide. Nevertheless, to further access the subtle details of the relevant quantum phases and to disentangle the complex interplay of spin, charge, and lattice degrees of freedom, experiments at x-ray synchrotron, muon, and neutron sources are often required. Various uniaxial pressure cells were optimized for different scattering geometries and successfully used, with designs ranging from differential thermal expansion<sup>31</sup> to one-screw compression<sup>22</sup> to an adaptation of anvil-type cells<sup>32</sup> without any transmission medium. A major drawback of these cells is that they only allow applying pressure *ex situ*, which is time consuming and inefficient.

Therefore, given the strong demand for measurement time optimization at large scale facilities, complex sample environments such as uniaxial pressure devices must be highly efficient and, hence, *in situ* tuning is the necessary approach. An additional, but relevant, advantage of the *in situ* system is that it allows the isothermal tuning of the uniaxial pressure. Moreover, the samples are often larger than those in lab-based measurements, which can further push the complexity of the design. So far, two approaches have been employed. To adapt the piezoelectric system to allow bigger displacements, a piezoelectric stack device with multiple elements was built<sup>33</sup> and successfully used in muon spin rotation/relaxation experiments.<sup>15,34</sup> Alternatively, copper bellows can be filled with pressurized helium gas to generate the force needed for manipulating the materials.<sup>35–37</sup> Although very successful, both of these approaches are of extensive complexity and require a nontrivial operation.

The device presented here is a new solution, based on simple operating principles, yet providing accurate application of pressure and the ability to apply force *in situ* at temperatures ranging from room temperature down to cryogenic temperatures. The device is also sufficiently compact to even fit into a cryomagnet, allowing for simultaneous tuning of temperature, magnetic field, and uniaxial pressure. The device is targeting the tuning of quantum materials introduced above, with relatively low requirements in applied strain,

but in turn, requires a very precise control of the strain to resolve changes at even subtle pressures inherent to this class of materials. For the same reasons, to accurately study subtle effects, the design of the device enables application of both tensile and compressive pressure, with the ability to easily access zero-pressure measurements for reference. Furthermore, the option to quickly exchange the pre-mounted samples and the availability of multiple modular sample holders optimize the precious measurement time at large scale facilities. Sections II–III outline the operating principle and the details of the device, followed by test measurements in Sec. IV showing the first results of the operational system.

## II. TECHNICAL IMPLEMENTATION OF THE DEVICE

### A. Force generation and transmission

A general overview of the apparatus is shown in Fig. 1. In order to achieve a precise control, the force in our device is generated using a motor linear actuator (MLA) with microstepping from Trinamic company (PD57-2-1161). The MLA allows for the smallest available rotational step size of  $0.00703^\circ$ , corresponding to a traveling distance of  $0.0195\text{ }\mu\text{m}$ . While this is already a fine step, for our purposes of a maximal strain of about 1% of a typical sample of  $\sim 2\text{ mm}$ , the full movement of  $0.02\text{ mm}$  corresponds to only  $\sim 1000$  steps.

To increase the resolution, additional spring disk packages are installed in series. They start deforming at low forces and, consequently, increase the effective linear movement. Moreover, this ensures that the force is applied gently after the engagement and preserves potentially fragile samples.

In our implementation, we use four standard EN 16983 disk springs in series, each of which plastically deforms by  $0.176\text{ mm}$  upon application of  $200\text{ N}$  force, which is the maximum anticipated value in the experiments. This, combined with extra deformation of the load cell ( $\sim 0.07\text{ mm}/200\text{ N}$ ), increases

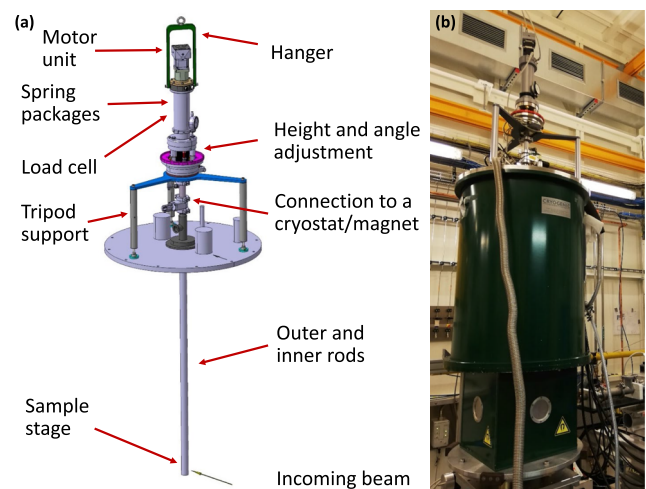


**FIG. 1.** The new uniaxial pressure device. (a) Main parts of the force generation and transmission elements of the pressure cell. (b) Pressure device positioned in a CRYOGENIC horizontal-10T cryomagnet on the P21.1 beamline in PETRA-III synchrotron at DESY.

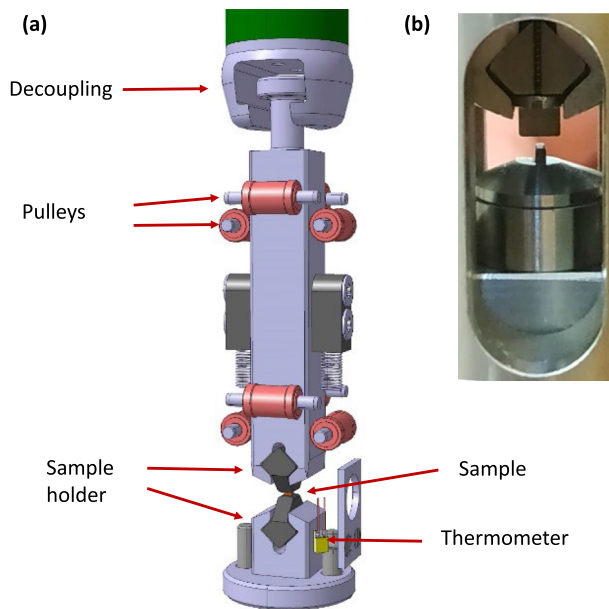


**FIG. 2.** Sample stage of the apparatus (a) showing the force transmission parts, thermometer, and sample positioned in the multi-directional holder. (b) A  $\text{La}_{2-x}\text{Ba}_x\text{CuO}_4$  sample installed for measurements at the P21.1 beamline, using a push-only sample holder.

the effective traveling distance up to  $\sim 0.8$  mm corresponding to  $\sim 40\,000$  microsteps, hence vastly improving the control of the precise load on the samples.

The 1.5 m long stainless steel (type 1.4404) push rod is connected to the sample stage (Fig. 2), where the force is transferred to the sample holders. In order to ensure a straight and efficient transmission of force through the sample stage, it is guided by a set of pulleys. The rod and the sample stage can be mechanically decoupled; there is a free movement of the rod of 3 mm, with respect to the sample stage. This decoupling mechanism protects from any buildup of strain upon temperature variation and enables true zero pressure reference measurements. In order to apply the tensile (compressive) strain, the rod has to be retracted (extended) until engagement. The moment of engagement can be traced via the load cell (see also below).

The sample stage terminates with the slots for sample holders as shown in Fig. 2. The square outside shape of the sample holders ensures the proper alignment for pushing and pulling operations, while transmitting the applied force efficiently. Apart from the constraint of the square fixation shape, the sample stage can accept a variety of sample holders, some of which are presented in Sec. II C and are readily adaptable for future implementations.

## B. Feedback and control

The applied force is measured using a load cell (see Fig. 1) by transducer techniques (MLP 50), which allows measuring loads of up to +220 N. In addition to the force measurement, the apparatus is measuring the temperature in the vicinity of the sample

(see Fig. 2) using a Cernox thin film resistance cryogenic temperature sensor (CX-SD-PACKAGE), which is read via a LakeShore-340 controller.

The software control is realized by employing the Frappy package<sup>38</sup> with a SECoP interface<sup>39</sup> on an embedded server board (PC Engines APU4D4). It enables processing the measured force and temperature values as well as sending commands to the motor to initiate or stop movement. For situations, when a constant-force measurement is required, a feedback loop can be enabled to compare the read force with the desired value and apply the corrective action using the motor. This mode is essential when a large temperature variation takes place during the measurement.

## C. Sample holders

The present apparatus is able to apply a compressive and tensile pressure, and consequently, the sample holders were designed to support both push and pull measurements. Moreover, the holders can be replaced quickly so that previously prepared and glued samples can be efficiently exchanged during the beamtime when measurement time is precious. The device is compatible with different types of sample holders. For example, in pull-only experiments, when sufficiently strong and easy-to-handle samples are available, they can be shaped into dogbones. We expect, however, that most of the samples would be glued into the holders, as has been successfully done in other cases.<sup>30,36</sup> The different types of holders can also be quickly changed by removing the bottom part of the sample stage.

Two sample holders, which were already successfully tested and deployed in experiments, are presented in Fig. 3. For the holder compatible with both pushing and pulling [Fig. 3(a)], the sample is glued to the inside tubes of the holders using epoxy. The cross section of the sample holder is displayed in the inset of the figure. After aligning the crystal within the sample holder, the gaps between the holder and the sample are filled with epoxy in a manner similar to the one reported in Ref. 30. To facilitate the transport and distribution of the

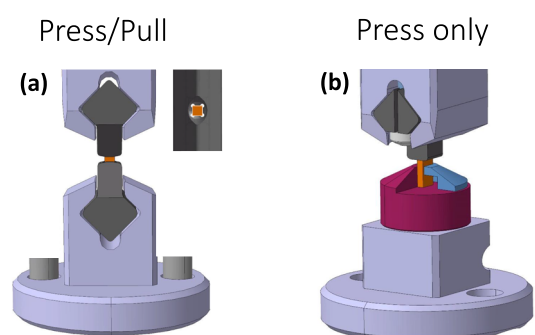


**FIG. 3.** Different sample holders that have been used with the uniaxial pressure device. (a) Sample holder with both push and pull capacity, with the inset showing the cross section of the holder and the sample. The gaps between the holder and the sample are filled with epoxy to transfer the force between the holder and the sample. The sample holder pictured in (b) is optimized for samples, where pushing only is needed. The empty space between the sample and the holder is filled with epoxy for stability.

epoxy and to increase the holding power, channels are added at the corners of the cavity. Then, the top and bottom sample holders are simultaneously slid into the square slots, which maintain the whole system straight.

For samples, where only pushing action is needed, a different holder shown in Fig. 3(b) can be used. The top part of the holder is replaced by a pusher, which is stabilized by screwing it into the sample stage. The bottom part has a versatile base, upon which various heads can be positioned, depending on the size of the sample and its properties. In the presented case, the sample (orange) is glued using epoxy to the bottom part of the sample. The bottom part of the sample can be rotated in order to access different parts of the reciprocal space, in case of a limited scattering angle of the sample environment.

### III. COMPATIBILITY WITH INSTRUMENTATION

The uniaxial device presented in this paper can be used in various scenarios but is particularly suited for experiments in a quasi-transmission geometry featuring small scattering angles, such as high energy (around 100 keV) x-ray diffraction and small angle neutron scattering (SANS) measurements. It is attached to the cryostat or magnet using a standard KF25 flange or using additional adapters when needed. While for small tilting angles, this provides enough support, upon further tilting, or for situations with long adapters, an additional tripod was designed to prevent the torque on the device (Fig. 1).

In order to make sure that the sample position could be modified inside the cryostat for centering and signal optimization purposes, a displacement unit is installed that can translate the device along the vertical direction with a range of 18 mm.

Moreover, there is an additional radial adjustment system to align the oriented sample with the available windows in the magnets and cryostats.

Control-wise, the instrument has been designed to work using the Sample Environment Automation (SEA) client-server software for controlling and monitoring sample environment devices at the Swiss Spallation Neutron Source SINQ. It has been further incorporated into the beamline control elements at the PETRA-III synchrotron using the PyTango device control framework.

### IV. EXPERIMENTAL TESTS

In order to test the operation of the device and to check the efficiency of the force transfer through the long distance of the apparatus, we have first measured the stress-strain curves of a steel mini dogbone ( $t = 0.5$  mm;  $d = 1.7$  mm) using the setup described here and comparing it with the measurement of exactly the same dogbone using a micro-tensile machine,<sup>40</sup> where the load cell is right next to the sample, which, in turn, is right next to the stepper motor. This allowed us to compare the readings of the load cells of the two systems at identical strain values. Because the experiment was performed in the pulling setup, it also allowed us to test the less common tensile pressure option. As shown in Fig. 4, the agreement is very good, verifying the efficient force transfer across the device.

Then, we tested the control system to ensure that correct forces are reached and that the feedback loop maintains a constant force.

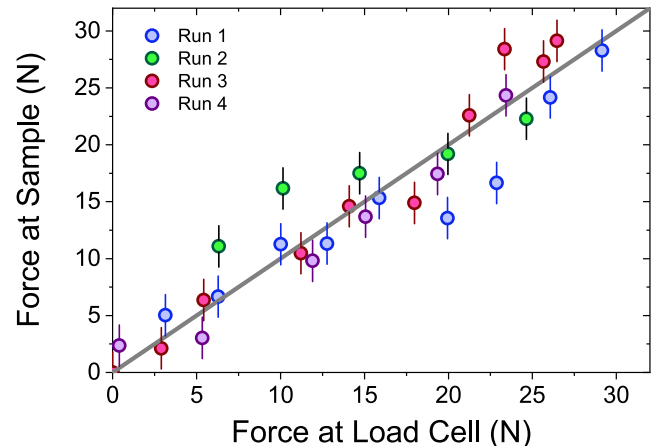


**FIG. 4.** Measurement of the efficiency of the force transmission. The abscissa shows the force values as read from the transducer, whereas the ordinate corresponds to the extracted force from the optical measurement of the length of a previously calibrated steel dogbone. Runs 1 and 3 are upon loading, and Runs 2 and 4 are upon releasing the force.

Figure 5 shows the loading curve for a force application during a real experiment at PETRA-III. As shown in the figure, the motor responds in an efficient manner both during the initial application and to compensate for the fluctuation in the force.

Having satisfied the requirement of an efficient force transfer and precise control, we then checked whether the crystals are continuously deformed up to high forces while on the P21.1 beamline at PETRA-III. We have investigated a pertinent case of the  $\text{La}_{2-x}\text{Ba}_x\text{CuO}_4$  system with  $x = 0.115$  under uniaxial compression.

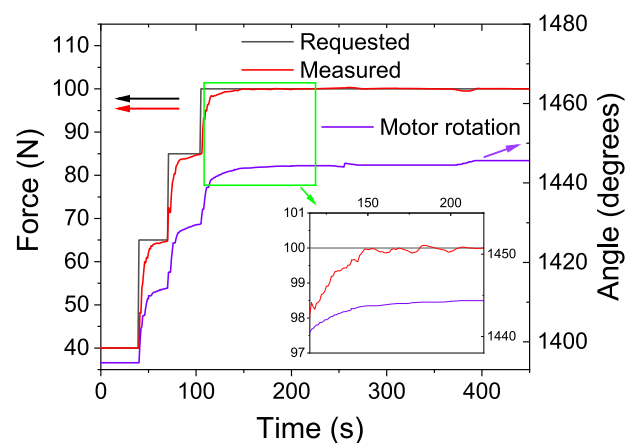


**FIG. 5.** Loading and control of the force application. Here, we show how the force is increased up to 100 N in three steps. The measured force (red line) traces the requested force value (black line) with a small time delay to ensure a gentle application of force. The motor (purple line) not only ensures the application of the force but also runs on a feedback loop to maintain a constant force value, the effect best seen in the inset, where we show a small time window indicated by the green box.



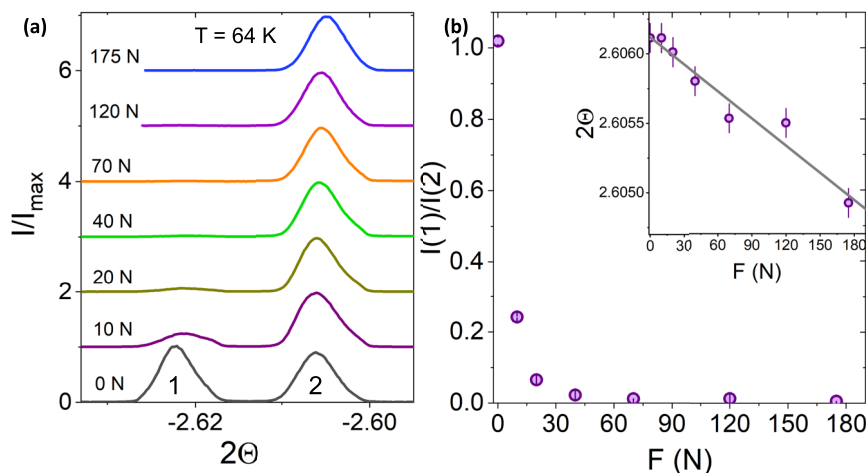


**FIG. 6.** Effect of uniaxial pressure on the structure of  $\text{La}_{1.885}\text{Ba}_{0.115}\text{CuO}_4$ . (a) Diffraction data on the structural peaks of  $\text{La}_{1.885}\text{Ba}_{0.115}\text{CuO}_4$  at different applied forces. The peaks labeled “1” and “2” correspond to different structural domains in the orthorhombic phase. The intensity of one of the peaks is suppressed due to detwinning, with the intensity ratio of the two peaks shown in (b). The scattering angle of the surviving peak continuously decreased, as expected for this geometry, and is plotted in the inset.

The full study of the properties under strain will be reported elsewhere;<sup>41</sup> here, we present the demonstration of the uniaxial pressure effects in the orthorhombic phase at 64 K. The crystal was positioned with tetragonal  $[0, 0, 1]$  and  $[1, 1, 0]$  directions spanning the scattering plane, and the pressure was applied perpendicular to the plane. The sample surface upon which the force was applied was rectangular with dimensions of  $0.65 \times 1.60 \text{ mm}^2$ . Therefore, the maximum pressure we could reach with our device was 0.2 GPa, which covers the full region of interest identified in the  $\mu\text{SR}$  study.<sup>15</sup> Figure 6 shows how the structural peaks arising from the  $(1, 1, 0)$  tetragonal peak respond to the application of the uniaxial pressure.

Since the material is orthorhombic at these temperatures, two domains [corresponding to  $(2, 0, 0)$  and  $(0, 2, 0)$  peaks in the orthorhombic notation] can be expected as shown in Fig. 6(a) with no applied force. The uniaxial pressure has long been used to structurally detwin orthorhombic crystals, and it is also observed in our case with one of the peaks losing the intensity very quickly, also plotted in Fig. 6(b). In addition, we track the scattering angle of the surviving peak as we increase the applied force [the inset of Fig. 6(b)]. As expected, when measuring the peak perpendicular to the applied force (i.e., in the expanding direction), we observe a reduction in the scattering angle.

Our measurements demonstrate that the force can be continuously applied with a high precision and the structure of the crystals is efficiently modified, enabling the tuning of the properties of the material under investigation, in this case, the  $\text{La}_{2-x}\text{Ba}_x\text{CuO}_4$  system with  $x = 0.115$ .

## V. SUMMARY

In summary, we have designed and commissioned a new *in situ* uniaxial pressure device for x-ray and neutron scattering experiments, specifically tailored for the investigation of quantum matter at low temperatures and high magnetic fields. In particular, the design of the sample holder is highly flexible and can be adapted to support various sample requirements. The control system designed for the system can be easily integrated into the control stack of

large-scale research facilities. Taken together, the device can be easily used in a wide range of experimental situations.

## ACKNOWLEDGMENTS

This project received funding from the European Union’s Horizon 2020 research and innovation program under the Marie Skłodowska-Curie Grant Agreement No. 884104 (No. PSIFELLOW-III-3i). G.S. acknowledges the funding from the Chalmers X-Ray and Neutron Initiatives (CHANS). Y.S. acknowledges the funding from the Swedish Research Council (VR) through a Starting Grant (Grant No. Dnr.2017-05078) and from the Area of Advance-Material Sciences from Chalmers University of Technology. T.A. was supported by JSPS KAKENHI through Grant No. 19H01841. J.K., Q.W., and J.C. acknowledge the support from the Swiss National Science Foundation (Grant No. 200021\_188564). J.K. is further supported by the Ph.D. fellowship from the German Academic Scholarship Foundation. We acknowledge DESY (Hamburg, Germany), a member of the Helmholtz Association HGF, for the provision of experimental facilities. Parts of this research were carried out at the beamline P21.1 of the PETRA-III synchrotron. The beamtime was allocated for the long-term project proposal II-20190002 EC and a regular Proposal No. I-20210712 EC.

## AUTHOR DECLARATIONS

### Conflict of Interest

The authors have no conflicts to disclose.

### Author Contributions

**G. Simutis:** Data curation (equal); Formal analysis (lead); Investigation (lead); Methodology (equal); Project administration (equal); Validation (equal); Visualization (equal); Writing – original draft (lead); Writing – review & editing (equal). **A. Bollhalder:** Conceptualization (equal); Formal analysis (equal); Investigation (equal); Methodology (lead). **M. Zolliker:** Software (lead). **J. Küspert:** Data

curation (equal); Formal analysis (equal); Investigation (equal). **Q. Wang:** Data curation (equal); Formal analysis (equal); Investigation (equal); Visualization (equal). **D. Das:** Data curation (equal); Investigation (equal). **F. Van Leeuwen:** Data curation (equal); Formal analysis (equal); Investigation (equal); Methodology (equal). **O. Ivashko:** Data curation (equal); Formal analysis (equal); Investigation (equal); Methodology (equal); Resources (equal). **O. Gutowski:** Data curation (equal); Formal analysis (equal); Methodology (equal); Resources (equal); Software (equal). **J. Philippe:** Formal analysis (equal); Investigation (equal); Methodology (equal); Software (equal). **T. Kracht:** Formal analysis (equal); Investigation (equal); Methodology (equal); Software (equal). **P. Glaevec:** Investigation (equal); Methodology (equal); Software (equal). **T. Adachi:** Data curation (equal); Formal analysis (equal); Investigation (equal); Methodology (equal); Supervision (equal). **M. v. Zimmermann:** Data curation (equal); Formal analysis (equal); Investigation (equal); Methodology (equal); Supervision (equal). **S. Van Petegem:** Investigation (equal); Methodology (equal). **H. Luetkens:** Data curation (equal); Formal analysis (equal); Investigation (equal); Methodology (equal); Visualization (equal). **Z. Guguchia:** Data curation (equal); Formal analysis (equal); Investigation (equal); Methodology (equal); Supervision (equal); Visualization (equal). **J. Chang:** Conceptualization (equal); Data curation (equal); Formal analysis (equal); Funding acquisition (equal); Investigation (equal); Methodology (equal); Project administration (equal); Resources (equal); Supervision (equal). **Y. Sassa:** Conceptualization (equal); Funding acquisition (equal); Project administration (equal); Resources (equal); Supervision (equal). **M. Bartkowiak:** Conceptualization (equal); Funding acquisition (equal); Investigation (equal); Methodology (equal); Project administration (equal); Resources (equal); Supervision (equal). **M. Janoschek:** Conceptualization (equal); Formal analysis (equal); Funding acquisition (equal); Investigation (equal); Methodology (equal); Project administration (equal); Resources (equal); Supervision (equal); Writing – review & editing (equal).

## DATA AVAILABILITY

The data that support the findings of this study are available from the corresponding author upon reasonable request.

## REFERENCES

- Y. Tokura, M. Kawasaki, and N. Nagaosa, “Emergent functions of quantum materials,” *Nat. Phys.* **13**, 1056–1068 (2017).
- F. Giustino, J. H. Lee, F. Trier, M. Bibes, S. M. Winter, R. Valentí, Y.-W. Son, L. Taillefer, C. Heil, A. I. Figueroa, B. Plaçais, Q. Wu, O. V. Yazyev, E. P. A. M. Bakkers, J. Nygård, P. Forn-Díaz, S. De Franceschi, J. W. McIver, L. E. F. F. Torres, T. Low, A. Kumar, R. Galceran, S. O. Valenzuela, M. V. Costache, A. Manchon, E.-A. Kim, G. R. Schleder, A. Fazzio, and S. Roche, “The 2021 quantum materials roadmap,” *J. Phys.: Mater.* **3**, 042006 (2020).
- R. Cava, N. de Leon, and W. Xie, “Introduction: Quantum materials,” *Chem. Rev.* **121**, 2777–2779 (2021).
- K. Head-Marsden, J. Flick, C. J. Ciccarino, and P. Narang, “Quantum information and algorithms for correlated quantum matter,” *Chem. Rev.* **121**, 3061–3120 (2021).
- M. Vojta, “Quantum phase transitions,” *Rep. Prog. Phys.* **66**, 2069–2110 (2003).
- S. Sachdev and B. Keimer, “Quantum criticality,” *Phys. Today* **64**, 29–35 (2011).
- D. J. Scalapino, “A common thread: The pairing interaction for unconventional superconductors,” *Rev. Mod. Phys.* **84**, 1383–1417 (2012).
- K. Umeo, T. Igaue, H. Chyono, Y. Echizen, T. Takabatake, M. Kosaka, and Y. Uwatoko, “Uniaxial-stress induced magnetic order in CeNiSn,” *Phys. Rev. B* **60**, R6957–R6960 (1999).
- S.-I. Ikeda, N. Shirakawa, T. Yanagisawa, Y. Yoshida, S. Koikegami, S. Koike, M. Kosaka, and Y. Uwatoko, “Uniaxial-pressure induced ferromagnetism of enhanced paramagnetic  $\text{Sr}_3\text{Ru}_2\text{O}_7$ ,” *J. Phys. Soc. Jpn.* **73**, 1322–1325 (2004).
- J.-H. Chu, H.-H. Kuo, J. G. Analytis, and I. R. Fisher, “Divergent nematic susceptibility in an iron arsenide superconductor,” *Science* **337**, 710–712 (2012).
- A. Chacon, A. Bauer, T. Adams, F. Rucker, G. Brandl, R. Georgii, M. Garst, and C. Pfleiderer, “Uniaxial pressure dependence of magnetic order in  $\text{MnSi}$ ,” *Phys. Rev. Lett.* **115**, 267202 (2015).
- D. O. Brodsky, M. E. Barber, J. A. N. Bruin, R. A. Borzi, S. A. Grigera, R. S. Perry, A. P. Mackenzie, and C. W. Hicks, “Strain and vector magnetic field tuning of the anomalous phase in  $\text{Sr}_3\text{Ru}_2\text{O}_7$ ,” *Sci. Adv.* **3**, e1501804 (2017).
- T. Kissikov, R. Sarkar, M. Lawson, B. T. Bush, E. I. Timmons, M. A. Tanatar, R. Prozorov, S. L. Bud’ko, P. C. Canfield, R. M. Fernandes, and N. J. Curro, “Uniaxial strain control of spin-polarization in multicomponent nematic order of  $\text{BaFe}_2\text{As}_2$ ,” *Nat. Commun.* **9**, 1058 (2018).
- P. Liu, M. L. Klemm, L. Tian, X. Lu, Y. Song, D. W. Tam, K. Schmalzl, J. T. Park, Y. Li, G. Tan, Y. Su, F. Bourdarot, Y. Zhao, J. W. Lynn, R. J. Birgeneau, and P. Dai, “In-plane uniaxial pressure-induced out-of-plane antiferromagnetic moment and critical fluctuations in  $\text{BaFe}_2\text{As}_2$ ,” *Nat. Commun.* **11**, 5728 (2020).
- Z. Guguchia, D. Das, C. N. Wang, T. Adachi, N. Kitajima, M. Elender, F. Brückner, S. Ghosh, V. Grinenko, T. Shiroka, M. Müller, C. Mudry, C. Baines, M. Bartkowiak, Y. Koike, A. Amato, J. M. Tranquada, H. H. Klauss, C. W. Hicks, and H. Luetkens, “Using uniaxial stress to probe the relationship between competing superconducting states in a cuprate with spin-stripe order,” *Phys. Rev. Lett.* **125**, 097005 (2020).
- C. W. Nicholson, M. Rumo, A. Pulkkinen, G. Kremer, B. Salzmann, M.-L. Motas, B. Hildebrand, T. Jaouen, T. K. Kim, S. Mukherjee, K. Ma, M. Muntwiler, F. O. von Rohr, C. Cacho, and C. Monney, “Uniaxial strain-induced phase transition in the 2D topological semimetal  $\text{IrTe}_2$ ,” *Commun. Mater.* **2**, 25 (2021).
- C. W. Hicks, D. O. Brodsky, E. A. Yelland, A. S. Gibbs, J. A. N. Bruin, M. E. Barber, S. D. Edkins, K. Nishimura, S. Yonezawa, Y. Maeno, and A. P. Mackenzie, “Strong increase of  $T_c$  of  $\text{Sr}_2\text{RuO}_4$  under both tensile and compressive strain,” *Science* **344**, 283–285 (2014).
- A. Steppke, L. Zhao, M. E. Barber, T. Scaffidi, F. Jerzembeck, H. Rosner, A. S. Gibbs, Y. Maeno, S. H. Simon, A. P. Mackenzie, and C. W. Hicks, “Strong peak in  $T_c$  of  $\text{Sr}_2\text{RuO}_4$  under uniaxial pressure,” *Science* **355**, eaaf9398 (2017).
- V. Sunko, E. Abarca Morales, I. Marković, M. E. Barber, D. Milosavljević, F. Mazzola, D. A. Sokolov, N. Kikugawa, C. Cacho, P. Dudin, H. Rosner, C. W. Hicks, P. D. C. King, and A. P. Mackenzie, “Direct observation of a uniaxial stress-driven Lifshitz transition in  $\text{Sr}_2\text{RuO}_4$ ,” *npj Quantum Mater.* **4**, 46 (2019).
- H.-H. Kim, S. M. Souliou, M. E. Barber, E. Lefrançois, M. Minola, M. Tortora, R. Heid, N. Nandi, R. A. Borzi, G. Garbarino, A. Bosak, J. Porras, T. Loew, M. König, P. J. W. Moll, A. P. Mackenzie, B. Keimer, C. W. Hicks, and M. Le Tacon, “Uniaxial pressure control of competing orders in a high-temperature superconductor,” *Science* **362**, 1040–1044 (2018).
- H.-H. Kim, E. Lefrançois, K. Kummer, R. Fumagalli, N. B. Brookes, D. Betto, S. Nakata, M. Tortora, J. Porras, T. Loew, M. E. Barber, L. Braicovich, A. P. Mackenzie, C. W. Hicks, B. Keimer, M. Minola, and M. Le Tacon, “Charge density waves in  $\text{YBa}_2\text{Cu}_3\text{O}_{6.67}$  probed by resonant x-ray scattering under uniaxial compression,” *Phys. Rev. Lett.* **126**, 037002 (2021).
- J. Choi, Q. Wang, S. Jöhr, N. B. Christensen, J. Küspert, D. Bucher, D. Biscette, M. H. Fischer, M. Hücker, T. Kurosawa, N. Momono, M. Oda, O. Ivashko, M. v. Zimmermann, M. Janoschek, and J. Chang, “Unveiling unequivocal charge stripe order in a prototypical cuprate superconductor,” *Phys. Rev. Lett.* **128**, 207002 (2022).
- Q. Wang, K. von Arx, D. G. Mazzone, S. Mustafi, M. Horio, J. Küspert, J. Choi, D. Bucher, H. Wo, J. Zhao, W. Zhang, T. C. Asmara, Y. Sassa, M. Månsson, N. B. Christensen, M. Janoschek, T. Kurosawa, N. Momono, M. Oda, M. H. Fischer, T. Schmitt, and J. Chang, “Uniaxial pressure induced stripe order rotation in  $\text{La}_{1.88}\text{Sr}_{0.12}\text{CuO}_4$ ,” *Nat. Commun.* **13**, 1795 (2022).

- <sup>24</sup>G. Simutis, J. Küspert, Q. Wang, J. Choi, D. Bucher, M. Boehm, F. Bourdarot, M. Bertelsen, C. N. Wang, T. Kurosawa, N. Momono, M. Oda, M. Månsson, Y. Sassa, M. Janoschek, N. B. Christensen, J. Chang, and D. G. Mazzone, “Single-domain stripe order in a high-temperature superconductor,” *Commun. Phys.* **5**, 296 (2022).
- <sup>25</sup>M. E. Kamminga, K. M. L. Krighaar, A. T. Rømer, L. Å. Sandberg, P. P. Deen, M. Boehm, G. D. Gu, J. M. Tranquada, and K. Lefmann, “Evolution of magnetic stripes under uniaxial stress in  $\text{La}_{1.885}\text{Ba}_{0.115}\text{CuO}_4$  studied by neutron scattering,” *arXiv:2203.00558* (2022).
- <sup>26</sup>F. Bourdarot, N. Martin, S. Raymond, L.-P. Regnault, D. Aoki, V. Taufour, and J. Flouquet, “Magnetic properties of  $\text{URu}_2\text{Si}_2$  under uniaxial stress by neutron scattering,” *Phys. Rev. B* **84**, 184430 (2011).
- <sup>27</sup>D. A. S. Kaib, S. Biswas, K. Riedl, S. M. Winter, and R. Valentí, “Magnetoelastic coupling and effects of uniaxial strain in  $\alpha\text{-RuCl}_3$  from first principles,” *Phys. Rev. B* **103**, L140402 (2021).
- <sup>28</sup>Y. Nii, T. Nakajima, A. Kikkawa, Y. Yamasaki, K. Ohishi, J. Suzuki, Y. Taguchi, T. Arima, Y. Tokura, and Y. Iwasa, “Uniaxial stress control of skyrmion phase,” *Nat. Commun.* **6**, 8539 (2015).
- <sup>29</sup>A. Fert, V. Cros, and J. Sampaio, “Skyrmions on the track,” *Nat. Nanotechnol.* **8**, 152–156 (2013).
- <sup>30</sup>C. W. Hicks, M. E. Barber, S. D. Edkins, D. O. Brodsky, and A. P. Mackenzie, “Piezoelectric-based apparatus for strain tuning,” *Rev. Sci. Instrum.* **85**, 065003 (2014).
- <sup>31</sup>T. J. Boyle, M. Walker, A. Ruiz, E. Schierle, Z. Zhao, F. Boschini, R. Sutarto, T. D. Boyko, W. Moore, N. Tamura, F. He, E. Weschke, A. Gozar, W. Peng, A. C. Komarek, A. Damascelli, C. Schüßler-Langeheine, A. Frano, E. H. da Silva Neto, and S. Blanco-Canosa, “Large response of charge stripes to uniaxial stress in  $\text{La}_{1.475}\text{Nd}_{0.4}\text{Sr}_{0.125}\text{CuO}_4$ ,” *Phys. Rev. Res.* **3**, L022004 (2021).
- <sup>32</sup>R. Edberg, I. M. B. Bakke, H. Kondo, L. Ø. Sandberg, M. L. Haubro, M. Guthrie, A. T. Holmes, J. Engqvist, A. Wildes, K. Matsuhira, K. Lefmann, P. P. Deen, M. Mito, and P. Henelius, “Effects of uniaxial pressure on the spin ice  $\text{Ho}_2\text{Ti}_2\text{O}_7$ ,” *Phys. Rev. B* **102**, 184408 (2020).
- <sup>33</sup>S. Ghosh, F. Brückner, A. Nikitin, V. Grinenko, M. Elender, A. P. Mackenzie, H. Luetkens, H.-H. Klauss, and C. W. Hicks, “Piezoelectric-driven uniaxial pressure cell for muon spin relaxation and neutron scattering experiments,” *Rev. Sci. Instrum.* **91**, 103902 (2020).
- <sup>34</sup>V. Grinenko, S. Ghosh, R. Sarkar, J.-C. Orain, A. Nikitin, M. Elender, D. Das, Z. Guguchia, F. Brückner, M. E. Barber, J. Park, N. Kikugawa, D. A. Sokolov, J. S. Bobowski, T. Miyoshi, Y. Maeno, A. P. Mackenzie, H. Luetkens, C. W. Hicks, and H.-H. Klauss, “Split superconducting and time-reversal symmetry-breaking transitions in  $\text{Sr}_2\text{RuO}_4$  under stress,” *Nat. Phys.* **17**, 748–754 (2021).
- <sup>35</sup>C. Pfeleiderer, E. Bedin, and B. Salce, “He activated loading device for low temperature uniaxial and anvil cell pressure experiments,” *Rev. Sci. Instrum.* **68**, 3120–3124 (1997).
- <sup>36</sup>D. M. Fobes, Y. Luo, N. León-Brito, E. D. Bauer, V. R. Fanelli, M. A. Taylor, L. M. DeBeer-Schmitt, and M. Janoschek, “Versatile strain-tuning of modulated long-period magnetic structures,” *Appl. Phys. Lett.* **110**, 192409 (2017).
- <sup>37</sup>L. Degiorgi, “Optical fingerprints of nematicity in iron-based superconductors,” *Front. Phys.* **10** (2022).
- <sup>38</sup>See <https://github.com/SampleEnvironment/frappy> for the description and the python code for the Frappy package.
- <sup>39</sup>K. Kiefer, L. Rossa, F. Wutzler, N. Ekström, A. Pettersson, E. Faulhaber, and M. Zolliker, “An introduction to SECoP—The sample environment communication protocol,” *J. Neutron Res.* **21**(3–4), 181–195 (2019).
- <sup>40</sup>H. Van Swygenhoven, B. Schmitt, P. M. Derlet, S. Van Petegem, A. Cervellino, Z. Budrovic, S. Brandstetter, A. Bollhalder, and M. Schild, “Following peak profiles during elastic and plastic deformation: A synchrotron-based technique,” *Rev. Sci. Instrum.* **77**, 013902 (2006).
- <sup>41</sup>Z. Guguchia *et al.*, “Effective control of the stripe-ordered cuprate phase diagram using uniaxial-stress” (unpublished).